Hindawi
Mathematical Problems in Engineering
Volume 2024, Article ID 7012424, 10 pages
https://doi.org/10.1155/2024/7012424

Research Article

Seismic Reliability Analysis of an Excavation Slope Based on Direct Probability Integral Method

Junguo Han,[1] Yuanmin Yang,[2] Muzi Du,[3] and Rui Pang[2,4]

[1]*CCCC Third Harbor Engineering Co., Ltd., Shanghai 200032, China*
[2]*School of Infrastructure Engineering, Dalian University of Technology, Dalian 116024, China*
[3]*CCCC Water Transportation Consultants Co., Ltd., Beijing 100007, China*
[4]*State Key Laboratory of Coastal and Offshore Engineering, Dalian University of Technology, Dalian 116024, China*

Correspondence should be addressed to Rui Pang; pangrui@dlut.edu.cn

Received 28 December 2023; Revised 13 January 2024; Accepted 18 March 2024; Published 30 March 2024

Academic Editor: Adriana del Carmen Téllez-Anguiano

China, situated in the circum-Pacific seismic belt, experiences frequent seismic activity and faces diverse geological conditions, making structural stability of paramount importance, especially under seismic conditions. The majority of current earthquake generation methods do not consider the nonstationary nature of earthquakes. This paper introduces a spectral representation-random function model for generating nonstationary earthquakes, effectively simulating stochastic seismic ground motion. Furthermore, traditional slope stability analysis methods are deterministic and incapable of providing probabilistic assessments of slope instability. Therefore, this paper proposes a unified framework for static and dynamic structural reliability analysis based on the direct probability integration method, quantifying the impact of stochastic seismic ground motion on the dynamic reliability of slope stability. Finally, the proposed methods are applied to an excavation slope in Nanjing, using sliding displacement and safety factors as evaluation criteria to study the reliability of the slope under the influence of stochastic seismic events.

1. Introduction

Earthquakes are known for their instantaneous and unpredictable nature, causing significant impacts on ground buildings. China is situated within the circum-Pacific seismic belt, one of the world's most active seismic zones, characterized by frequent earthquakes and diverse geological conditions [1]. As a result, seismic safety considerations are significant for all types of engineering projects, including slopes [2, 3]. Slope instability could lead to infrastructure and environmental damage, severely impacting surrounding environments and economic activities. For instance, the catastrophic Wenchuan earthquake in 2008 triggered enormous mountain landslides, causing approximately 20,000 fatalities directly [4]. Similarly, the 2014 Ludian earthquake in Yunnan caused the largest Hongshiyan landslide, blocking the Niulan River and creating a landslide dam, posing even greater risks [5]. Historically, earthquakes have been identified as a major cause of landslides. Therefore, the implementation of seismic analysis for slope is essential to ensure the durability and resilience of structure, reduce potential losses, and enhance the overall seismic safety of engineering projects.

When conducting slope stability analysis, traditional methods such as the pseudo-static method, stress deformation analysis, and permanent displacement analysis are commonly employed [6, 7]. These are deterministic analysis methods, assuming that all input parameters are known with certainty, although soil parameters and external factors may have high uncertainties. However, these factors, which significantly impact slope stability, are not fully considered in deterministic analysis [8–10]. Moreover, deterministic analysis cannot provide probabilistic assessments or risk analyses of slope instability, which is a crucial aspect of engineering decision-making. Over the years, with advancements in risk and reliability analysis methods, engineers have increasingly utilized probabilistic methods to address uncertainties and changes [11–15], thus providing a more precise evaluation of slope stability [16–18].

Among all methods for structural reliability analysis, Monte Carlo simulation (MCS) stands out as an established technique directly applicable to the response analysis of

nonlinear random structures [19, 20]. However, this method requires a significant number of random sampling and simulation operations, resulting in high computational costs. Therefore, Li and Chen [21] and Li [22] proposed an innovative probability density evolution method (PDEM) for dynamic response analysis of nonlinear stochastic structures. PDEM demands fewer samples than MCS, thereby enhancing computational efficiency and solution accuracy [23–26]. Nevertheless, when employing PDEM to solve the generalized density evolution equation, a virtual stochastic process is introduced, which requires substantial computation and additional numerical calculations. To address this issue, Chen and Yang [27, 28] developed a unified framework for static and dynamic structural reliability analysis based on the direct probability integration method (DPIM). This method eliminates the complex challenges of solving partial differential equations and simplifies the integral equation through the use of the Dirac function smooth approximation method, making it more suitable for addressing complex problems.

The generation of earthquakes is crucial in seismic analysis for slope stability. Methods for generating stochastic ground motions can be classified into two categories: stationary and nonstationary ground motions. Historically, most ground motion simulation methods overlooked the nonstationary characteristics of ground motions [29]. For instance, the power spectrum model is typically built based on stationary ergodic assumptions. However, a significant number of historical earthquake records reveal clear amplitude and frequency nonstationary characteristics in ground motions. Consequently, a model capable of synthesizing the acceleration time history of nonstationary ground motions is required.

In this paper, we utilize the spectral expression-random function model to generate a nonstationary earthquake and employ DPIM for the reliability analysis of the slope. This paper is organized as follows: Section 2 outlines the principles of DPIM and the methodology for using DPIM to evaluate the dynamic reliability of the structure; Section 3 details the ground motion simulation method utilized in this paper, generating 144 random ground motions to validate the accuracy of this approach; Section 4 provides the engineering background, finite element model (FEM), and material parameter values for an excavation slope in Nanjing; Section 5 evaluates the reliability of the slope based on two indicators, namely sliding displacements and safety factor. The structure of the paper is shown in Figure 1.

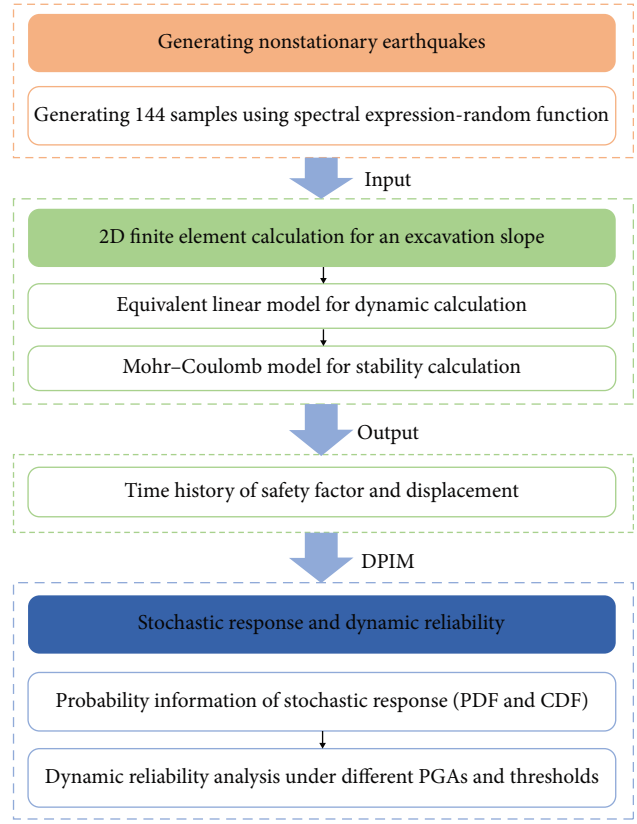

Figure 1: The structure of the paper.

2. DPIM

The DPIM method, as proposed by Chen and Yang [27], can calculate the failure probability in the random variable space without considering the failure domain and obtain the probability density function (PDF) of the structural response based on the probability density integral equation (PDIE).

Combined with the mapping function and the Dirac function variant formula, the PDIE of the dynamic stochastic system can be expressed as follows:

$$p_Y = \int_{-\infty}^{\infty} p_\Theta(\theta)\delta[y - g(\theta, t)]d\theta, \tag{1}$$

where y is the output vector, representing the response vector. $p_\Theta(\theta)$ means the PDF of the input random vector Θ; Ω_Θ is the sample space of the input random vector; $\delta(\blacksquare)$ is the Dirac delta function.

Equation (1) remains a challenging task. To address this, Chen and Yang [28] proposed the DPIM employing two distinct techniques: partitioning the input probability space and smoothing the Dirac delta function with the Gaussian function. This innovative approach effectively transforms the original integral equation into a concise numerical integration form, allowing the PDIE to be expressed as follows:

$$\begin{aligned} p_Y(y, t) &\cong \sum_{q=1}^{N} \left\{ \delta[y - g(\theta, t)] \int_{\Omega_{\Theta,q}} p_\Theta(\theta)d\theta \right\} \\ &\cong \sum_{q=1}^{N} \left\{ \frac{1}{\sqrt{2\pi}\sigma} e^{-[y-g(\theta_q,t)]^2/2\sigma^2} P_q \right\}, \end{aligned} \tag{2}$$

where the subscript "q" means the qth representative point. And θ is probability space; $\Omega_{\Theta,\mathrm{q}}$ is the representative area occupied by the qth representative point; N is the total number of representative points; σ is the smoothing parameter,

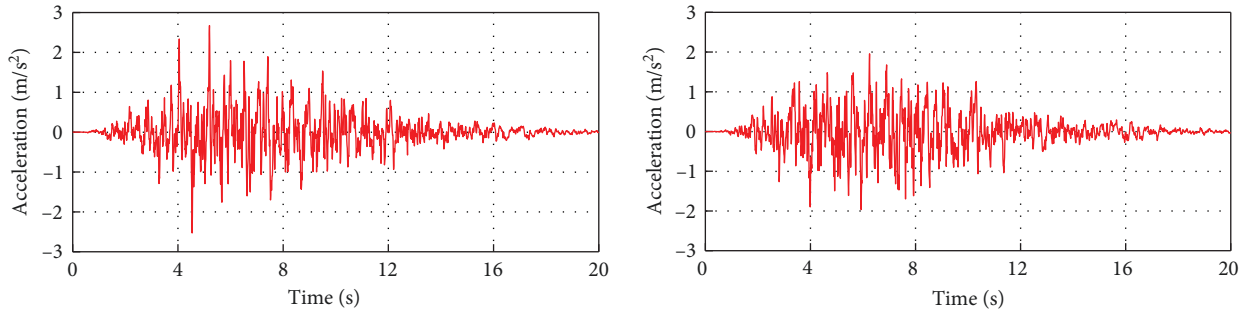

FIGURE 2: Acceleration time history of typical samples: (a) sample 1#; (b) sample 2#.

which is also the standard deviation of the Gaussian distribution; P represents the distribution probability.

In dynamical systems, reliability cannot be directly obtained from instantaneous PDFs with integrated performance functions. Therefore, the absorption condition (AC) method is used to calculate the time-varying reliability.

The formula for determining the failure probability of the qth representative point response using DPIM can be expressed as follows:

$$p_{q,f}(t) = P_q(t) \int_{-\infty}^{0} \frac{1}{\sqrt{2\pi}\sigma} e^{-\left[y-g\left(\theta_q,t\right)\right]^2/2\sigma^2} dy. \tag{3}$$

The concept behind the AC method is that the failure of the qth representative response at a specific moment will not persist into the subsequent moment. This process can be depicted by absorbing the failure probability to zero as follows:

$$p_{q,f}(t_i) = 0, z \in \Omega_{y,f} = \{z | g\left(\theta_q, t_i\right) \le 0. \tag{4}$$

And now, the remaining probability of the response at the qth moment can be replaced by the effective part of the previous moment $P_{q,s}(t_{i-1})$, i.e.,

$$p_q(t_i) = P_{q,s}(t_{i-1}) = P_q(t_{i-1}) \int_{0}^{\infty} \frac{1}{\sqrt{2\pi}\sigma} e^{-\left[y-g\left(\theta_q,t_{i-1}\right)\right]^2/2\sigma^2} dy. \tag{5}$$

Combined with DPIM, the PDF of the random response corresponding to the survival domain can be expressed as follows:

$$P_{Z,s}(z,t) = \sum_{q=1}^{N} \left\{ \frac{1}{\sqrt{2\pi}\sigma} e^{-\left[z-g\left(\theta_q,t\right)\right]^2/2\sigma^2} P_q(t) \right\}. \tag{6}$$

Therefore, the first passage reliability is obtained as follows:

$$P_s(t) = P_r\{z>0\} = \int_{0}^{\infty} P_{Z,s}(z,t) dz, \tag{7}$$

where Z is the structural performance function. The failure probability can be expressed as follows:

$$P_f(t) = 1 - P_s(t). \tag{8}$$

3. Stochastic Earthquake Simulation Method

Based on the generalized Clough–Penzien power spectrum model [30], this paper adopts a random function to simulate stochastic earthquakes, referred to as nonstationary earthquakes, based on spectral expression-random function. The acceleration of a nonstationary stochastic earthquake with a zero mean can be calculated by the following:

$$\ddot{X}_g(t) = \sum_{k=1}^{N} \sqrt{2S_{\ddot{X}_g}(t,\omega_k)\Delta\omega} [\cos(\omega_k t) X_k + \sin(\omega_k t) Y_k], \tag{9}$$

where $\omega = k\Delta\omega$; $S_{\ddot{X}_g}$ is two-sided power spectral density function, and X_k and Y_k ($k = 1, 2, \ldots, N$) are a set of standard orthogonal random vectors, determined as follows:

Let's assume that any two sets of standard orthogonal random variables $\overline{X}_n$ and $\overline{Y}_n$ ($n = 1, 2, \ldots, N$) can be represented as functions of two independent random variables Θ_1 and Θ_2, namely random functions as follows:

$$\begin{cases} \overline{X}_n = \mathrm{cas}(n\Theta_1) \\ \overline{Y}_n = \mathrm{cas}(n\Theta_2) \end{cases}, \tag{10}$$

where $\mathrm{cas}(t) = \sin(t) + \cos(t)$ is the Hartley orthogonal basic function, and the random variables Θ_1 and Θ_2 are obtained by number-theoretical method and obey the uniform distribution on the interval $(0, 2\pi)$. After a certain deterministic mapping, $\{\overline{X}_n, \overline{Y}_n\}$ become the standard orthogonal basic random variables $\{X_k, Y_k\}$ required by Equation (9) and can be determined uniquely.

In this paper, we generated 144 acceleration time series, each with a duration of 20 s and featuring maximum peak ground acceleration (PGA) values of 0.2, 0.3, and 0.4 g. Taking 0.3 g PGA as an example, two samples are illustrated in Figure 2. Additionally, Figure 3 compares all 144 generated samples with the target values, demonstrating a good fit.

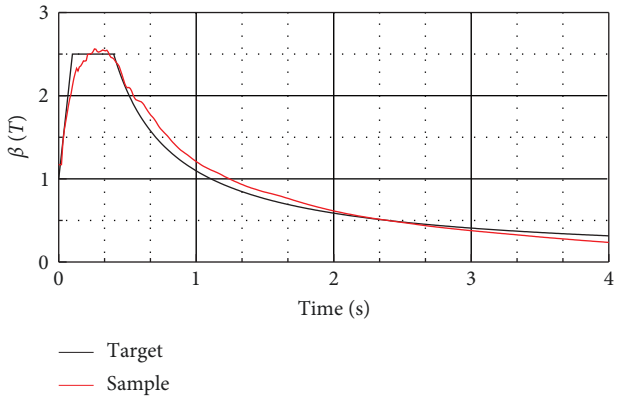

Figure 3: Comparison of the samples and the target.

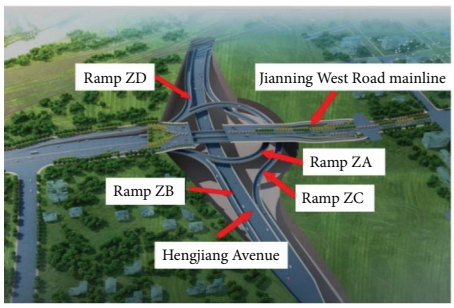

Figure 4: Project location map (from the company that built the project).

4. Establishment of Slope Model

4.1. FEM of Slope. This study explores an excavation in Area V of the main line of Jianning West Road in Nanjing, China. The 2D finite element method is employed to analyze the dynamic reliability of the layered soil slope. The project begins at the intersection of Xingpu Road and Jiangbei Expressway in Jiangbei New District, and its design endpoint is near the intersection of Jianning West Road and Rehe Road, spanning a total length of 6.801 km, as depicted in Figure 4.

The construction site is situated on the terrace along the left bank of the Yangtze River, characterized by a flat terrain. Based on the collected survey data, the stratigraphic distribution of the site is relatively uniform, with the lithology remaining stable throughout. Furthermore, according to the regional geological report and the Site Seismic Safety Assessment Report, the vicinity of the proposed project hosts an inactive fault, and the most recent active faults near the project date back to the late Quaternary Middle Pleistocene.

The slope section of the excavation in Area V of the main line is illustrated in Figure 5. The excavation section has a length of 51.072 m, a height of 20.445 m, an excavation depth of 5.624 m, and a slope ratio of 1 : 1.5. The distribution of soil layers is presented in Figure 5, featuring three layers from top to bottom: silty clay, 3d13 silt, and 3d12 silt.

The GeoStudio software (GeoStudio 2021.4) was employed for both dynamic and stability analyses. The FEM unit length was set to 0.5 m, divided into 3,219 units and 3,362 nodes. The finite element mesh utilized 4-node quadrilateral and 3-node triangular solid elements.

In the initial static analysis of the layered soil slope, constraints were imposed horizontally and vertically on the model's bottom, while exclusively horizontally on the left and right boundaries. However, during the dynamic analysis, only the bottom x and y directions were constrained.

Distinct mechanical properties of soils were represented by various constitutive models. As the foundation soil is compacted, the equivalent linear model is employed to describe the soil layer of the excavation. Furthermore, the Mohr–Coulomb yield criterion is utilized to characterize the soil behavior under seismic conditions in the dynamic analysis.

4.2. Material Parameters. The material parameters shown in Table 1 were determined by field tests. Additionally, the correlation between damping ratio, shear modulus, and cyclic shear strain is illustrated in Figure 6.

5. Slope Stability Assessment

In this section, the slope stability assessment will be developed from two perspectives: slope sliding displacement and safety factor. For seismic calculations, three operational conditions have been designed, i.e., PGA of 0.2, 0.3, and 0.4 g. Here, we will illustrate the process using a PGA of 0.3 g as an example.

5.1. Reliability Analysis concerning Sliding Displacement. After an earthquake, the sliding displacement of slopes becomes a highly intuitive and crucial evaluation index. As illustrated in Figure 7, the time history of sliding displacement for the entire sample is presented. Notably, the majority of displacement occurs within the range of 0–0.1 m. On average, the displacement is generally less than 0.025 m. The criteria for seismic analysis of slopes and landslide risk assessment, as proposed by Jibson and Michael [31], classifies permanent displacement into four levels for seismic hazard landslide risk assessment: 0–1 cm (low), 1–5 cm (moderate), 5–15 cm (high), and >15 cm (very high). Considering this, it can be inferred that the slope presents a moderate risk of seismic hazard landslide at a PGA of 0.3 g.

The evaluation of slope stability based solely on mean values neglects the unique probabilities associated with each sample, rendering it an imprecise approach. Therefore, assessing slope stability from a probabilistic perspective offers a more comprehensive and precise methodology. The DPIM can capture the entire probability density process of sliding displacement. Figure 8(a) illustrates its interception of one of the typical time periods. It is observed that the section with the highest probability of sliding displacement during the ground motion period is distributed in the range of 0–0.1 m, aligning with the phenomenon observed in Figure 7. Additionally, the event occurs around 10 s, and the probability density gradually decreases over time, indicating a gentle evolution. This suggests that the damage caused by the earthquake is primarily concentrated in the intermediate stage, with the destructive effects gradually diminishing. By extracting the equivalent portion of the probability density evolution surface, the probability contour of sliding displacement can be obtained, as

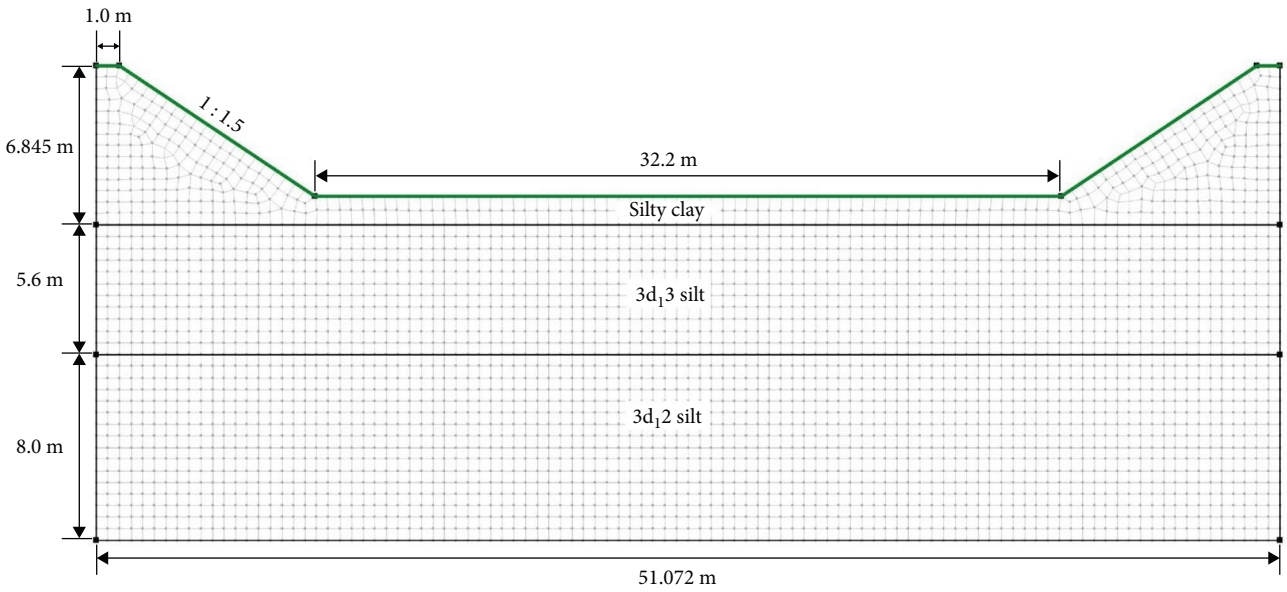

Figure 5: FEM and material zoning of slope.

Table 1: Slope soil parameters for the calculation.

Materials	C (kPa)	φ (°)	E (MPa)	γ (kN/m^3)	ν
Silty clay	11	11.8	17.5	17.4	0.3
3d$_1$3 silt	0	31.5	30	18	0.24
3d$_1$2 silt	0	31.5	30	20	0.24

Note. C denotes cohesion; φ denotes friction angle; E denotes elastic modulus; γ denotes unit weight; ν denotes Poisson's ratio.

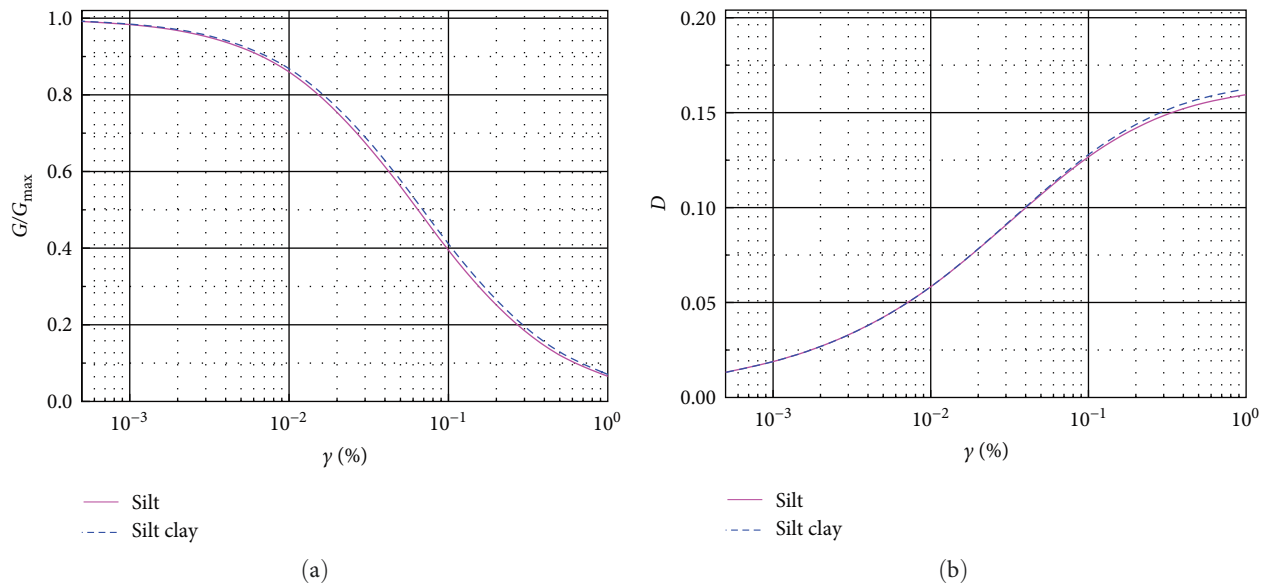

Figure 6: Relationship between cyclic shear strain and (a) damping ratio; (b) shear modulus of materials.

shown in Figure 8(b). This indicates that the probability density in the dynamic response gradually decreases over time.

Three specific time points (10, 12, and 16 s) have been chosen to extract slices from the probability density evolution surface, resulting in PDFs of displacement at these typical moments, as illustrated in Figure 9(a). Analysis indicates that the displacement response is most concentrated during the middle stage of the earthquake (10 s), with the

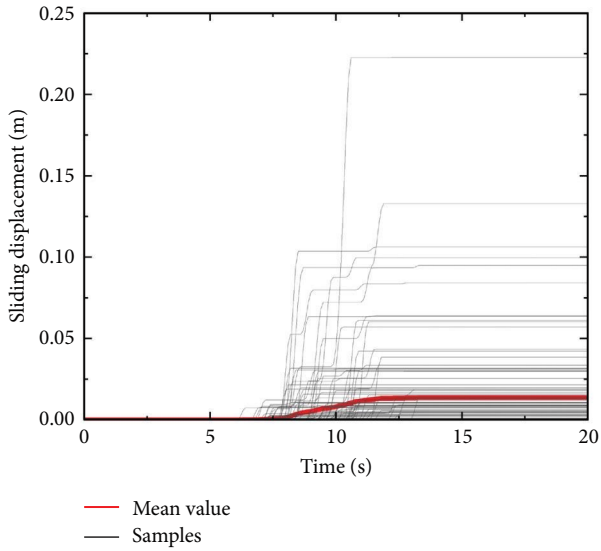

Figure 7: Time history of sliding displacement for 144 samples.

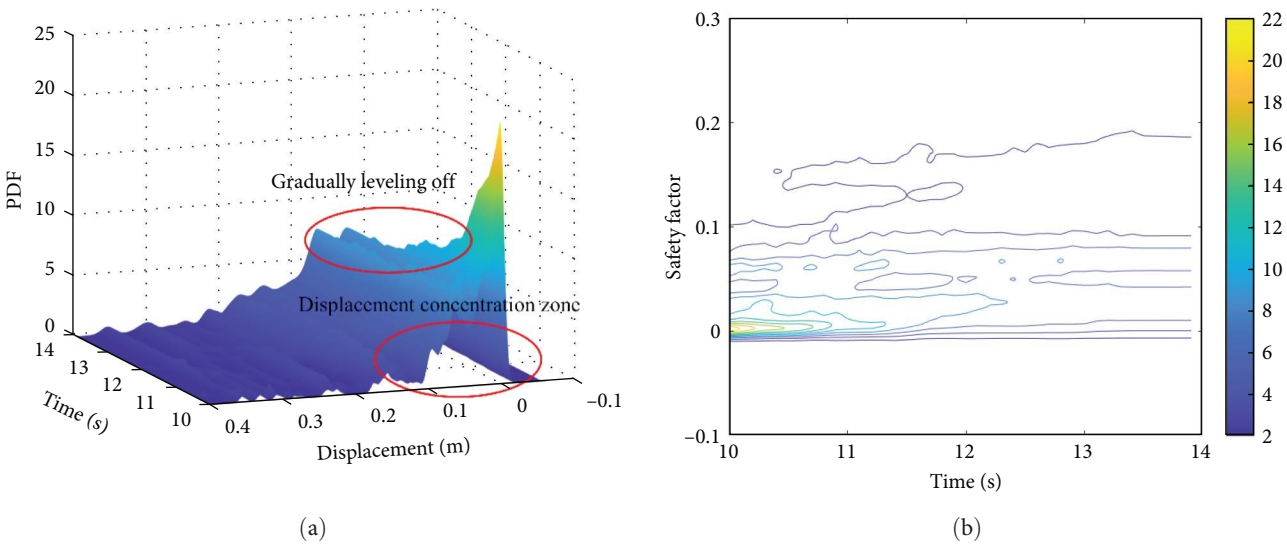

Figure 8: (a) Time history of probability density evolution and (b) probability contours at typical times of sliding displacement.

probability density primarily distributed in the range of 0–0.1 m, indicating a high risk for the structure. The response gradually expands over time, meaning the probability density decreases, signifying a diminishing impact of the earthquake in the later stages. The CDF was generated by integrating the PDF, as depicted in Figure 9(b), revealing a decrease in structural reliability over time.

The above analysis provides a probabilistic representation of typical times, followed by an assessment of slope reliability using the equivalent extreme value method. Subsequently, the time history of the maximum displacement probability for the entire sample is extracted. The PDF and CDF of the extreme displacement values are also illustrated in Figure 10. It is evident that structural reliability decreases to only 14% when the threshold value is set at 1 cm but increases to 35% when the threshold value reaches 5 cm. This indicates that as the threshold value increases, reflecting looser design conditions, the reliability improves.

The reliabilities of the slope under the other two conditions are outlined in Table 2. As evident from the table, the reliability of the slope without support remains high at only 0.2 g. However, it declines rapidly at a PGA of 0.3 g, emphasizing the critical need to enhance the slope's support during construction.

5.2. Reliability Analysis concerning Safety Factor. The primary objective of employing the limit equilibrium technique to assess slope stability is to determine the safety factor. The safety factor, determined based on the equilibrium conditions between the sliding and free surfaces for a given sliding

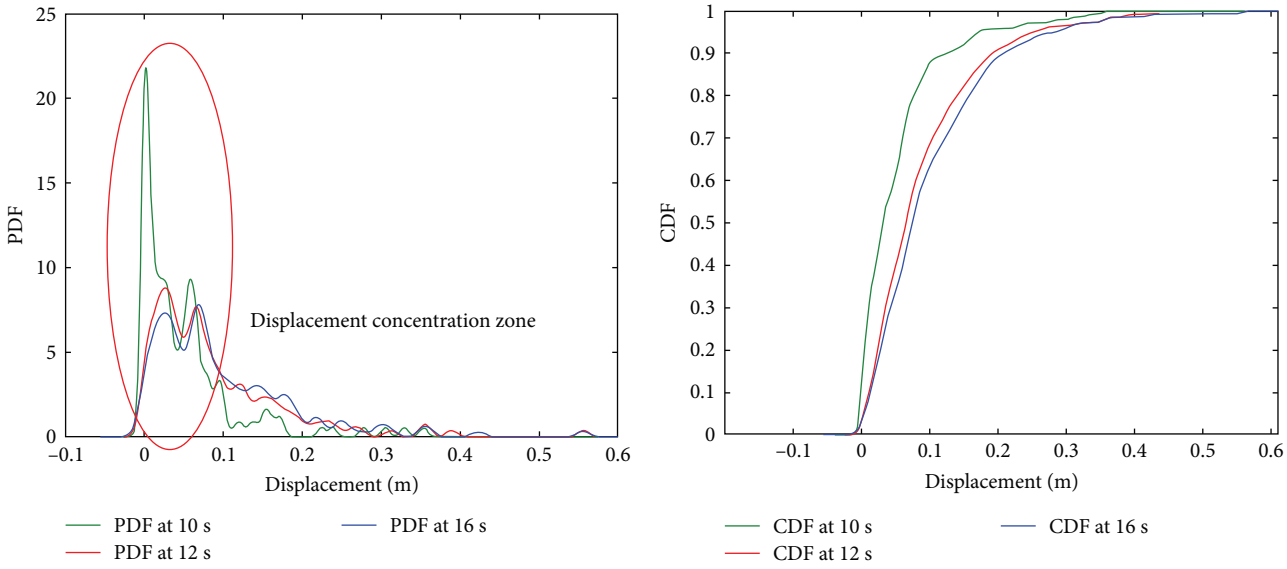

(a) (b)

Figure 9: (a) PDF and (b) CDF of sliding displacement at typical times.

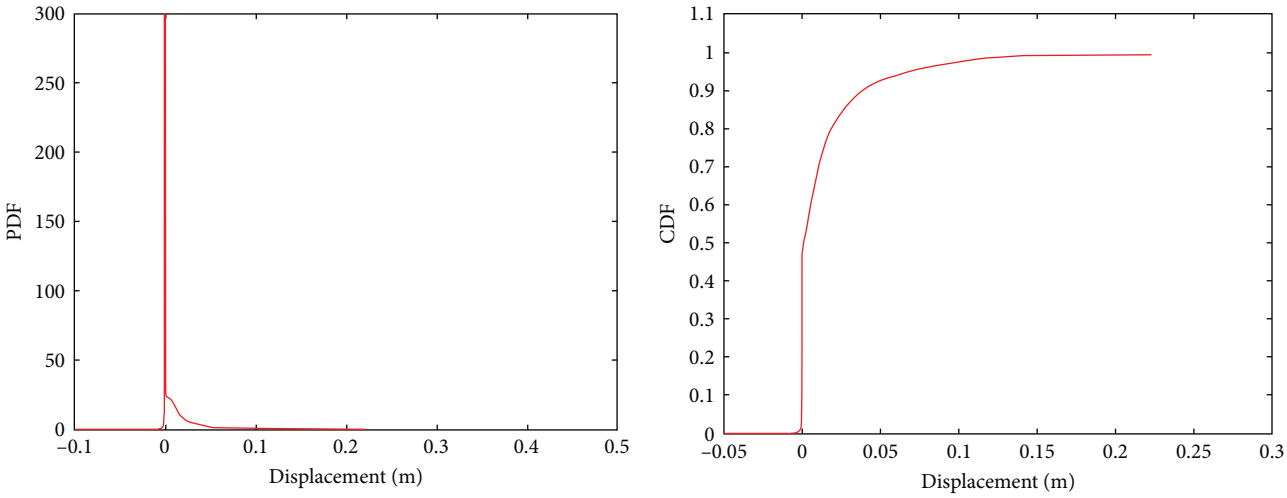

(a) (b)

Figure 10: (a) PDF and (b) CDF of the equivalent extreme value of sliding displacement for the whole sample.

Table 2: Dynamic reliability of slopes at different PGAs and thresholds.

Thresholds	PGA		
	0.2 g	0.3 g	0.4 g
1 cm	70%	14%	2%
5 cm	92.5%	35%	5%

surface, will be calculated in this section to assess the structural reliability [32].

In general, a lower safety factor indicates that the load-bearing capacity of the system or structure is closer to or less than the applied load, implying that the structure is less secure. The time history of the minimum safety factor for the entire sample is depicted in Figure 11, revealing that the majority of safety factors in the samples are greater than 1. Additionally, the mean value of the safety factor in the samples is also greater than 1.

Similar to an assessment based solely on sliding displacement, evaluating stability purely from a quantitative perspective oversimplifies the depiction of the structure's reliability. The evolution of the probability density at typical times using DPIM is illustrated in Figure 12(a). Figure 12 reveals that the highest probabilities of safety factors are distributed in the range of 1–2, indicating the structural safety. Moreover, the probability density evolution of the safety factor is less dramatic compared to that of sliding displacement and

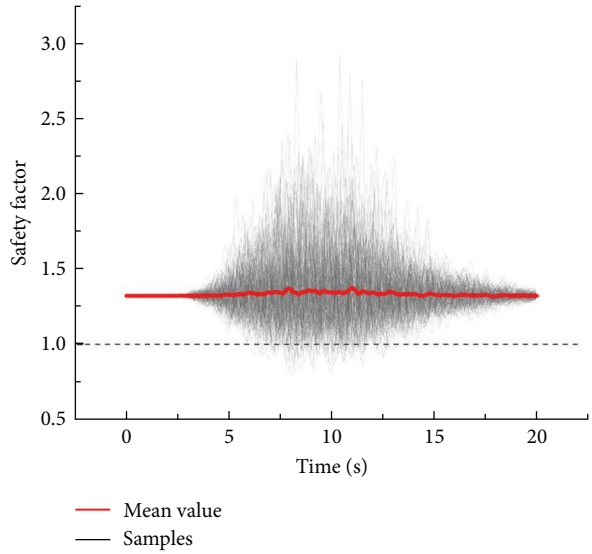

Figure 11: Time history of the minimum safety factor for the whole sample.

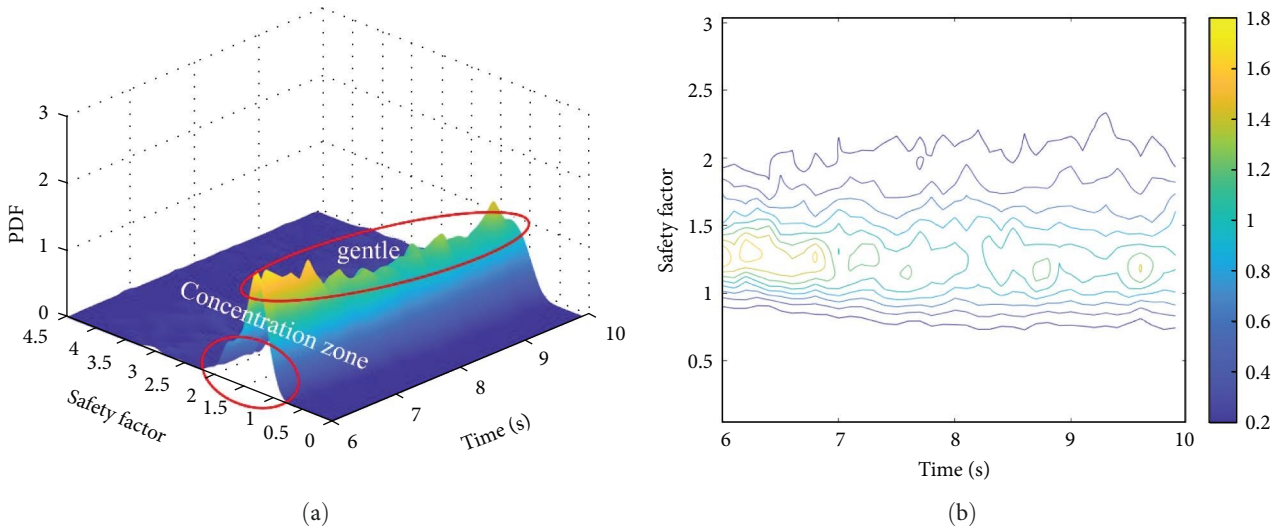

(a) (b)

Figure 12: (a) Time history of probability density evolution and (b) probability contours at typical times of the safety factor.

tends to be more gradual in general. This is due to the fact that the safety factor is in the form of a ratio, which provides a more stable value compared to random quantities, i.e., sliding displacement. This conclusion is further supported by the probability contours shown in Figure 12(b).

The probability density evolution surface at three typical times (10, 12, and 16 s) is selected for slicing to obtain the PDF curves, shown in Figure 13(a). It can be observed that the response of the safety factor is most concentrated during the middle stage of the earthquake, where the probability density is also most distributed, i.e., between 1 and 2. Then, the response gradually expands, indicating a gradual decrease in probability density. This indicates that the impact of the earthquake in the late stage is not as intense as that in the middle stage. The CDF is derived by integrating the PDF, as shown in Figure 13(b). From Figure 13, it is apparent that the structural reliability decreases with time, which is consistent with the conclusion drawn from the perspective of slip displacement.

6. Conclusions

In this paper, we tackle the prevailing challenges in contemporary slope seismic analysis, focusing on the issues of unreasonable earthquake generation and the absence of probabilistic information. We employ a spectral expression-random function model to simulate nonstationary ground motion and utilize the slope reliability analysis method based on the dynamic response

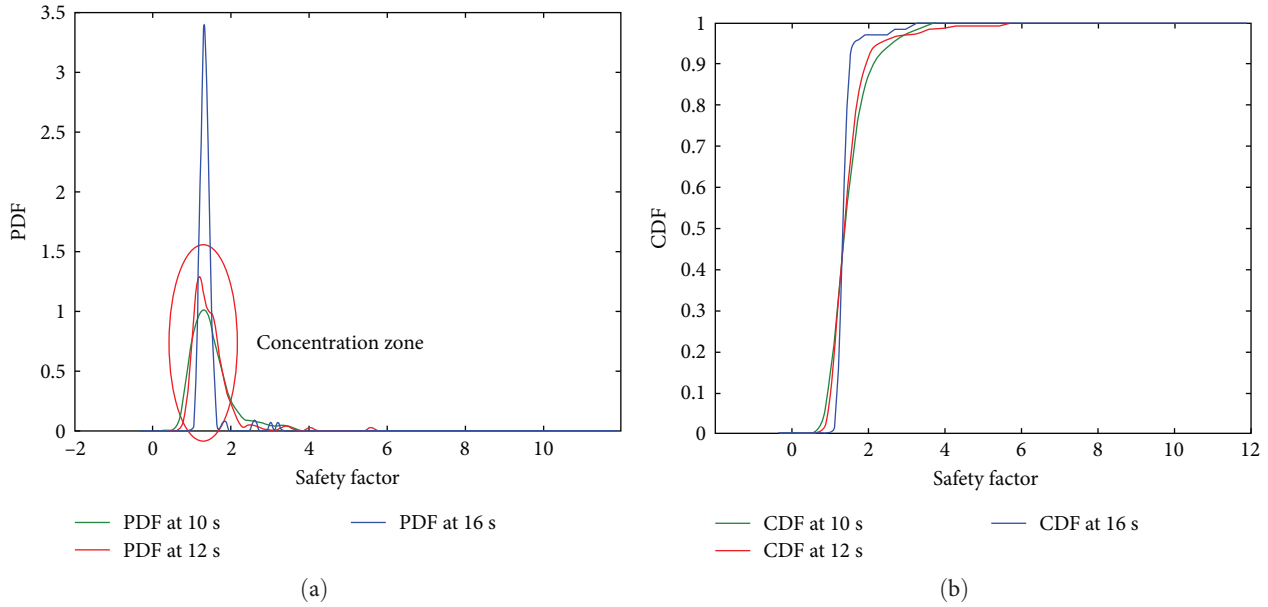

Figure 13: (a) PDF and (b) CDF of safety factor at typical times.

of DPIM to yield probability results. To illustrate the proposed methodology, we apply it to an excavation slope in Nanjing, and the conclusions drawn are as follows:

(1) The PDF evolution of sliding displacement is relatively more dynamic and pronounced, while that of the safety factor appears to be steadier and gentler. This may be attributed to the fact that slip, as a parameter quantifying displacement at a given point, is influenced by various variables susceptible to change, such as the moisture content and loads. Conversely, the PDF of the safety factor is influenced by relatively fixed variables, such as soil mechanical properties, which are less likely to change significantly in a short time.

(2) The probability density of the dynamic response of the structure is highest in the middle stage during an earthquake and then decreases, which indicates that the impact of the earthquake in the late stage is not as intense as in the middle stage. However, structure reliability decreases over time, as concluded from assessments of both sliding displacement and the safety factor.

(3) Structural reliability undergoes significant changes as the threshold diminishes; hence, it should be evaluated in consideration of project design demands.

However, our study has some limitations. The current model we established is 2D, and some studies suggest that 2D models may be somewhat conservative. This aspect requires further validation in future work.

Data Availability

Data supporting this research article are available on request.

Conflicts of Interest

The authors declare that they have no conflicts of interest.

Authors' Contributions

Rui Pang conceived the study and was in charge of overall direction and planning. Junguo Han devised the project and wrote the original manuscript with the support of Yuanmin Yang and Muzi Du. Yuanmin Yang developed the theoretical formalism, performed the analytic calculations, and performed the numerical simulations. Muzi Du edited and revised the manuscript as well as checked the results.

Acknowledgments

This work was supported by the National Natural Science Foundation of China (grant no. 52379117), the State Key Laboratory of Hydraulic Engineering Simulation and Safety Open Fund (HESS-2302), and the State Key Laboratory of Coastal and Offshore Engineering Young Scholars Innovation Fund (LY2301) and these financial supports are gratefully acknowledged.

References

[1] F. Huang, M. Li, Y. Ma et al., "Studies on earthquake precursors in China: a review for recent 50 years," *Geodesy and Geodynamics*, vol. 8, no. 1, pp. 1–12, 2017.

[2] Z. Ma, H. Liao, F. Dang, and Y. Cheng, "Seismic slope stability and failure process analysis using explicit finite element method," *Bulletin of Engineering Geology and the Environment*, vol. 80, no. 2, pp. 1287–1301, 2021.

[3] L. Lu, Z. Wang, X. Huang, B. Zheng, and K. Arai, "Dynamic and static combination analysis method of slope stability analysis during earthquake," *Mathematical Problems in Engineering*, vol. 2014, Article ID 573962, 14 pages, 2014.

[4] Y. Wan, Y. Gao, and F. Zhang, "Stability analysis of three-dimensional slopes considering the earthquake force direction," *Mathematical Problems in Engineering*, vol. 2018, Article ID 2381370, 11 pages, 2018.

[5] J. Luo, X. Pei, S. G. Evans, and R. Huang, "Mechanics of the earthquake-induced Hongshiyan landslide in the 2014 Mw 6.2 Ludian earthquake, Yunnan, China," *Engineering Geology*, vol. 251, pp. 197–213, 2019.

[6] R. W. Jibson, "Methods for assessing the stability of slopes during earthquakes—a retrospective. The next generation of research on earthquake-induced landslides," *Engineering Geology*, vol. 122, no. 1-2, pp. 43–50, 2011.

[7] Y. Huang and M. Xiong, "Dynamic reliability analysis of slopes based on the probability density evolution method," *Soil Dynamics and Earthquake Engineering*, vol. 94, pp. 1–6, 2017.

[8] Y. Li, R. Pang, and B. Xu, "Dynamic reliability analysis of three-dimensional slopes considering the spatial variability in soil parameters," *Structures*, vol. 56, Article ID 104977, 2023.

[9] Z.-Y. Chen and Z.-Q. Liu, "Stochastic seismic lateral deformation of a multi-story subway station structure based on the probability density evolution method," *Tunnelling and Underground Space Technology*, vol. 94, Article ID 103114, 2019.

[10] R. Pang, Y. Zhou, G. Chen, M. Jing, and D. Yang, "Stochastic mainshock-aftershock simulation and its applications in dynamic reliability of structural systems via DPIM," *Journal of Engineering Mechanics*, vol. 149, no. 1, Article ID 04022096, 2023.

[11] A. Johari, S. Mousavi, and A. H. Nejad, "A seismic slope stability probabilistic model based on Bishop's method using analytical approach," *Scientia Iranica*, vol. 22, no. 3, pp. 728–741, 2015.

[12] Y. Huang and M. Xiong, "Probability density evolution method for seismic liquefaction performance analysis of earth dam," *Earthquake Engineering & Structural Dynamics*, vol. 46, no. 6, pp. 925–943, 2017.

[13] X.-Y. Cao, D.-C. Feng, and M. Beer, "A KDE-based non-parametric cloud approach for efficient seismic fragility estimation of structures under non-stationary excitation," *Mechanical Systems and Signal Processing*, vol. 205, Article ID 110873, 2023.

[14] X.-Y. Cao, D.-C. Feng, and M. Beer, "Consistent seismic hazard and fragility analysis considering combined capacity-demand uncertainties via probability density evolution method," *Structural Safety*, vol. 103, Article ID 102330, 2023.

[15] Q. Yang, B. Zhu, and T. Hiraishi, "Probabilistic evaluation of the seismic stability of infinite submarine slopes integrating the enhanced Newmark method and random field," *Bulletin of Engineering Geology and the Environment*, vol. 80, no. 3, pp. 2025–2043, 2021.

[16] A. Canal and M. Akin, "Assessment of rock slope stability by probabilistic-based slope stability probability classification method along highway cut slopes in Adilcevaz–Bitlis (Turkey)," *Journal of Mountain Science*, vol. 13, no. 11, pp. 1893–1909, 2016.

[17] R. Pang, B. Xu, Y. Zhou, and L. Song, "Seismic time-history response and system reliability analysis of slopes considering uncertainty of multi-parameters and earthquake excitations," *Computers and Geotechnics*, vol. 136, Article ID 104245, 2021.

[18] G. Wang, R. Pang, X. Yu, and B. Xu, "Permanent displacement reliability analysis of soil slopes subjected to mainshock-aftershock sequences," *Computers and Geotechnics*, vol. 153, Article ID 105069, 2023.

[19] M. Shinozuka, "Monte Carlo solution of structural dynamics," *Computers & Structures*, vol. 2, no. 5-6, pp. 855–874, 1972.

[20] Y. Lu, R. Pang, M. Du, and B. Xu, "Simulation of non-stationary ground motions and its applications in high concrete faced rockfill dams via direct probability integral method," *Engineering Structures*, vol. 298, Article ID 117034, 2024.

[21] J. Li and J.-B. Chen, "The probability density evolution method for dynamic response analysis of non-linear stochastic structures," *International Journal for Numerical Methods in Engineering*, vol. 65, no. 6, pp. 882–903, 2006.

[22] J. Li, "Probability density evolution method: background, significance and recent developments," *Probabilistic Engineering Mechanics*, vol. 44, pp. 111–117, 2016.

[23] D.-C. Feng, X.-Y. Cao, and M. Beer, "An enhanced PDEM-based framework for reliability analysis of structures considering multiple failure modes and limit states," *Probabilistic Engineering Mechanics*, vol. 70, Article ID 103367, 2022.

[24] D.-C. Feng, X.-Y. Cao, D. Wang, and G. Wu, "A PDEM-based non-parametric seismic fragility assessment method for RC structures under non-stationary ground motions," *Journal of Building Engineering*, vol. 63, Article ID 105465, 2023.

[25] Y. Huang, M. Xiong, and H. Zhou, "Ground seismic response analysis based on the probability density evolution method," *Engineering Geology*, vol. 198, pp. 30–39, 2015.

[26] B. Xu, R. Pang, and Y. Zhou, "Verification of stochastic seismic analysis method and seismic performance evaluation based on multi-indices for high CFRDs," *Engineering Geology*, vol. 264, Article ID 105412, 2020.

[27] G. Chen and D. Yang, "Direct probability integral method for stochastic response analysis of static and dynamic structural systems," *Computer Methods in Applied Mechanics and Engineering*, vol. 357, Article ID 112612, 2019.

[28] G. Chen and D. Yang, "A unified analysis framework of static and dynamic structural reliabilities based on direct probability integral method," *Mechanical Systems and Signal Processing*, vol. 158, Article ID 107783, 2021.

[29] G. Fan, L.-M. Zhang, J.-J. Zhang, and C.-W. Yang, "Time-frequency analysis of instantaneous seismic safety of bedding rock slopes," *Soil Dynamics and Earthquake Engineering*, vol. 94, pp. 92–101, 2017.

[30] R. W. Clough and J. Penzien, *Dynamics of structures*, McGraw-Hill, NY, USA, 1975.

[31] R. W. Jibson and J. A. Michael, "Maps showing seismic landslide hazards in Anchorage, Alaska," US Geological Survey Reston, VA, USA, 2009, 2009.

[32] Y. Zhao, Z.-Y. Tong, and Q. Lü, "Slope stability analysis using slice-wise factor of safety," *Mathematical Problems in Engineering*, vol. 2014, Article ID 712145, 7 pages, 2014.